



Computational Experiment in AeroAcoustics
September 21-24, 2016, Svetlogorsk, Russia

Computational aeroacoustic methods for industrial applications

Philippe Lafon

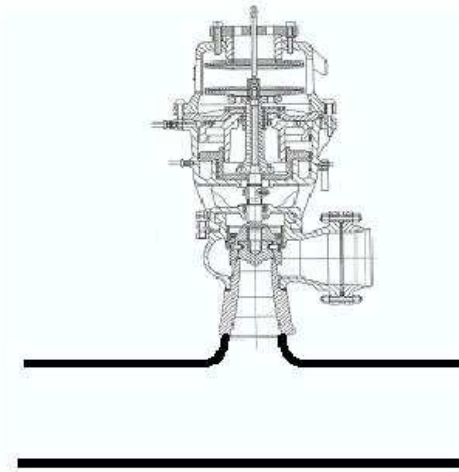
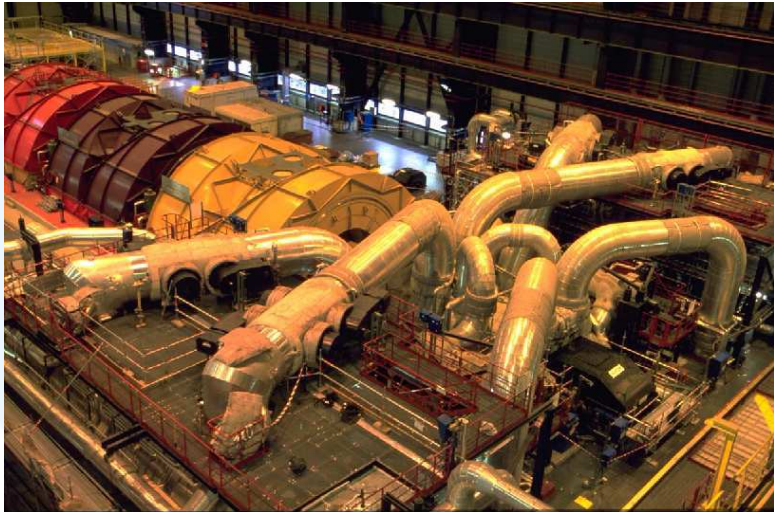
IMSIA

Institut des Sciences de la Mécanique et Applications Industrielles

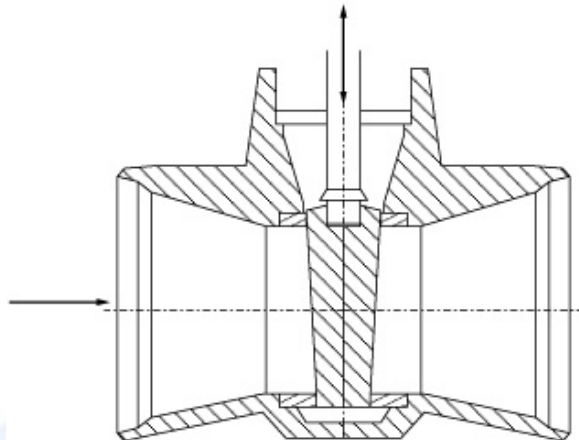




EDF industrial concerns



Safety valve



Gate valve

- Turbulent flows
- Compressible flows, shocks
- Coupling between acoustics and flow
- Complex geometries
- Acoustic propagation



Simulation approaches in aeroacoustics

In the past 25 years, different methods have been tested at EDF

- ◎ Hybrid methods
 - Lighthill analogy + RANS (Béchara et al. JASA 1994, Bailly et al. AIAAJ 1997)
 - Lighthill analogy + URANS, LES (Bastin et al. JFM 1997)
 - Linearized Euler equations + SNGR (Béchara et al. AIAAJ 1994)
- ◎ Numerical methods
 - Mac Cormack two and fourth order
 - TVD Harten/Yee (Lafon et al. AIAAP 1993)
 - DRP (support of the PhD Thesis of Bogey (2000) and Marsden (2005) at ECL)

This experience lead us to the development of a computational tool:
Code_Safari

PhD Thesis of Emmert (2007)
Emmert et al. Phys. of Fluids (2009)
Daude et al. Computers & Fluids 2012



Numerical algorithms for CAA

- ◎ Spatial discretization : optimized centered finite difference schemes

→Bogey & Bailly JCP 2004, Marsden et al. JCA 2005

- ◎ Time integration : explicit Runge-Kutta schemes

→Berland et al. Comp. & Fluids 2006

- ◎ Selective filtering : optimized centered low-pass filters

→Bogey & Bailly JCP 2004

- ◎ LES strategy : based on relaxation filtering

→Bogey & Bailly JFM 2009

- ◎ Shock capturing strategy : non linear adaptive second order filters

→Kim & Lee AIAA 2000, Bogey & Bailly JCP 2009



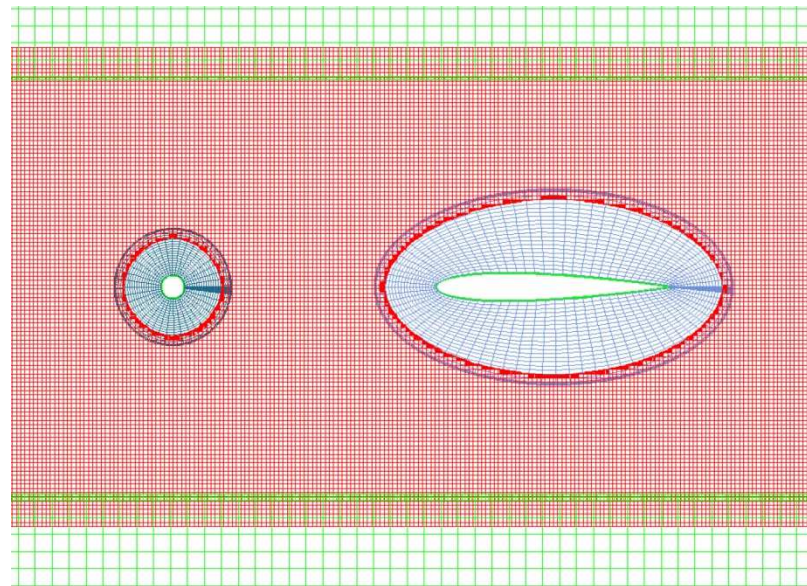
Multi-domain approach (1)

- ⊙ Use of composite overset-grid techniques with high-order interpolation procedures

→Delfs AIAA Paper 2001

- ⊙ Use of the free library *Overture* developed at Lawrence Livermore Laboratory

→Henshaw 1998

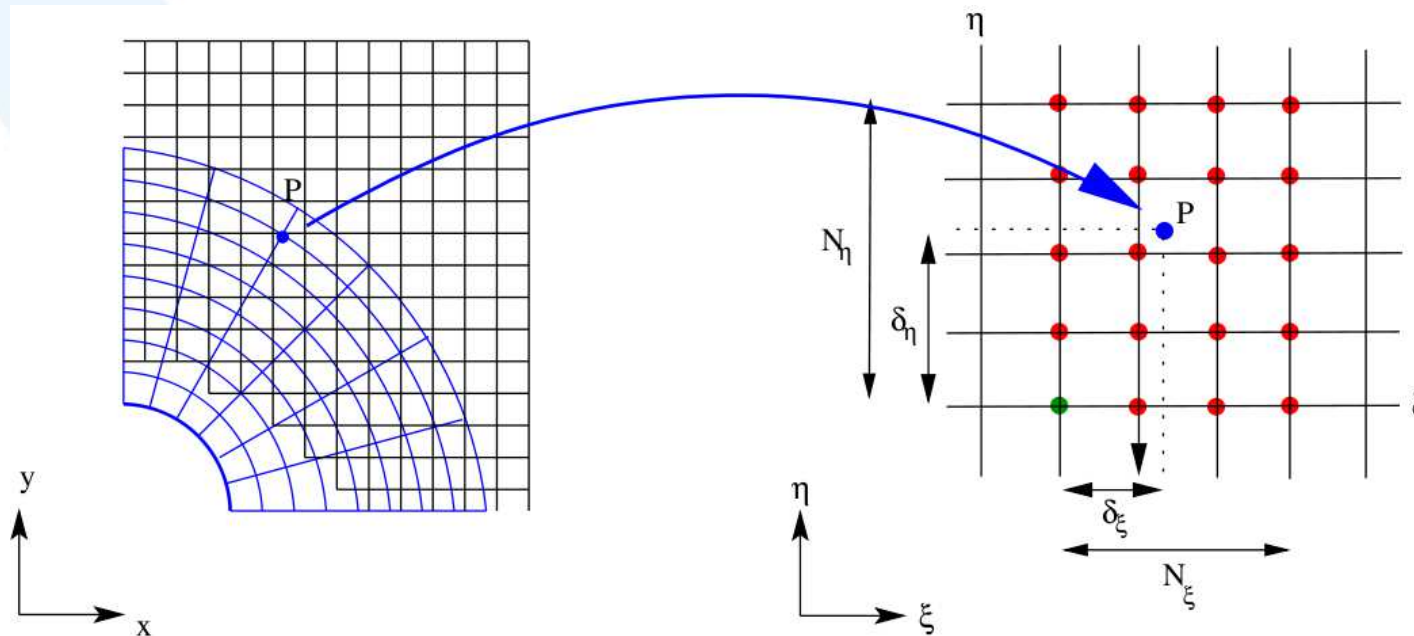




Multi-domain approach (2)

- Communication performed via high-order Lagrangian polynomial interpolation

→ Scott & Sherer JCP 2005, Desquesnes et al. JCP 2006,

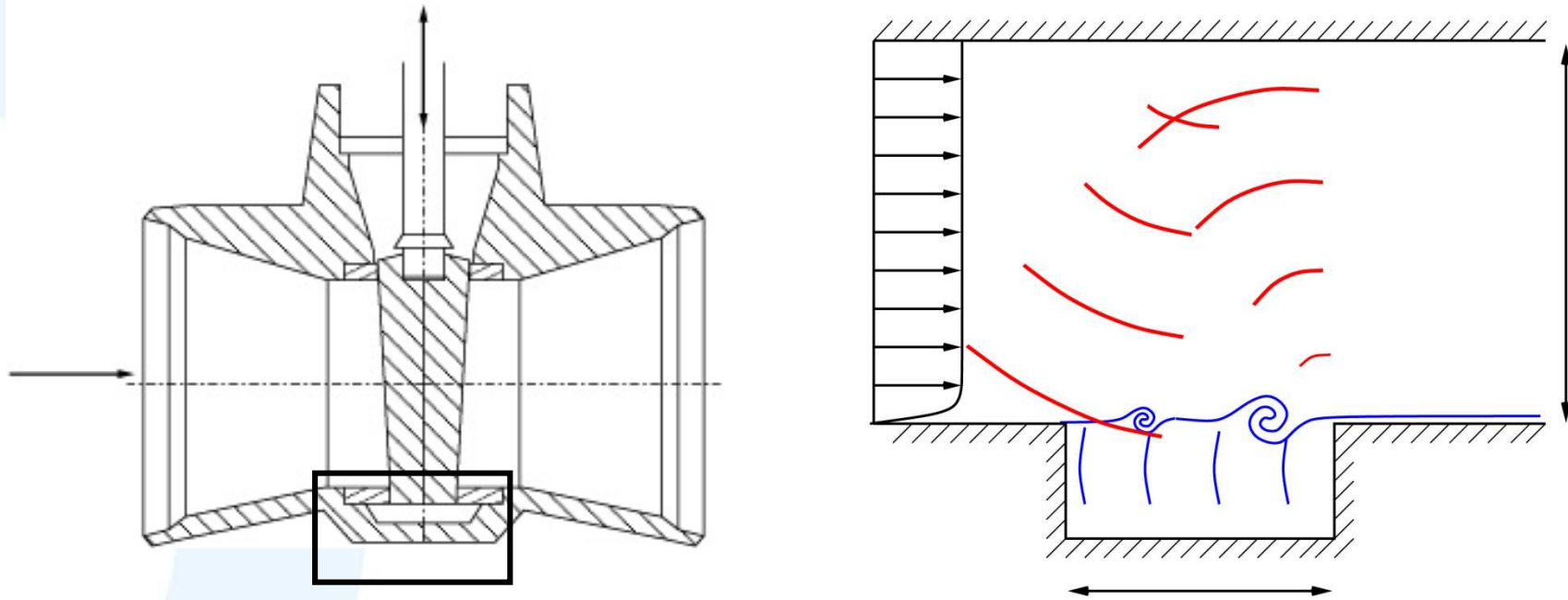


- Parallelization with MPI



Ducted cavity case (1/4)

- ⊙ « Test case » initiated because of a real problem on a gate valve



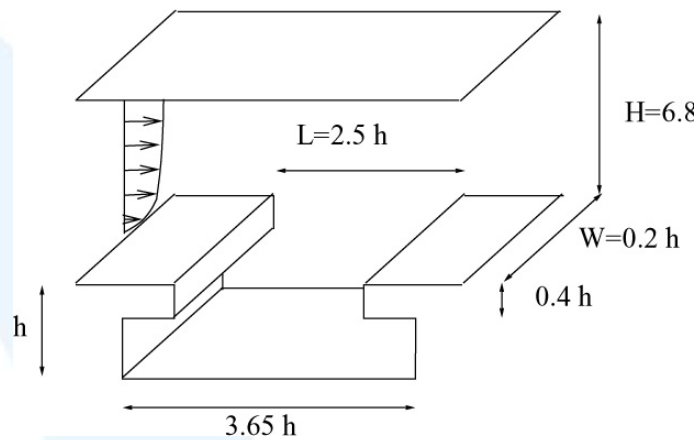
Lafon et al. JFS 2003

- ⊙ A strong whistling occurs when **hydrodynamic cavity modes** and **acoustic duct mode** match



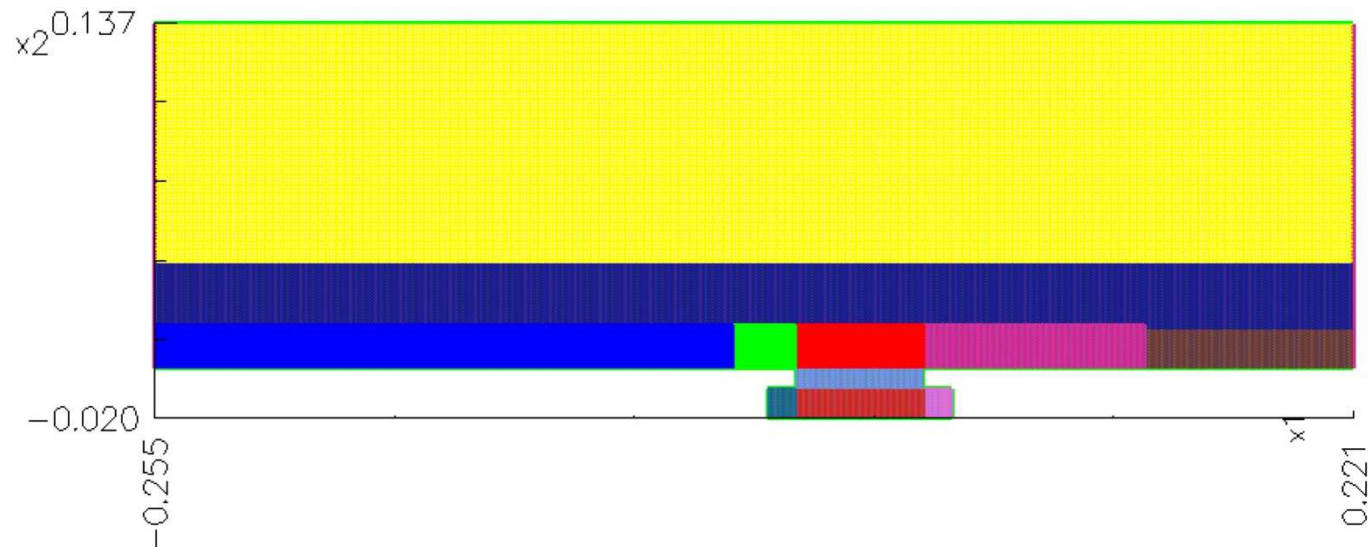
Ducted cavity case (2/4)

Sketch of the geometry



- 11 component grids
- 38 M points
- 206 procs
- $M = 0.18$
- $Re_H = 5.6 \cdot 10^5$

Overview of the composite grid

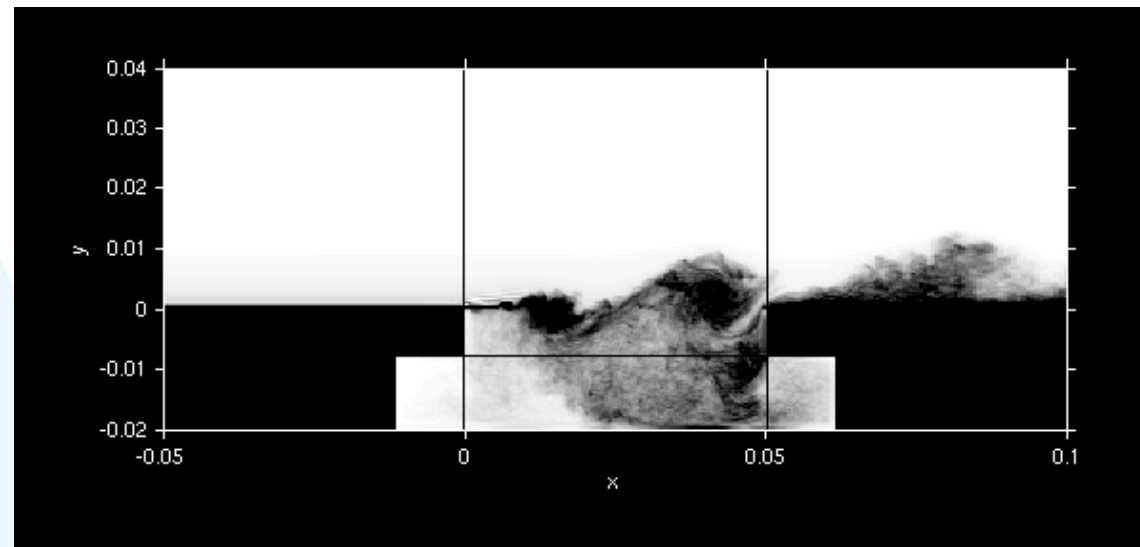




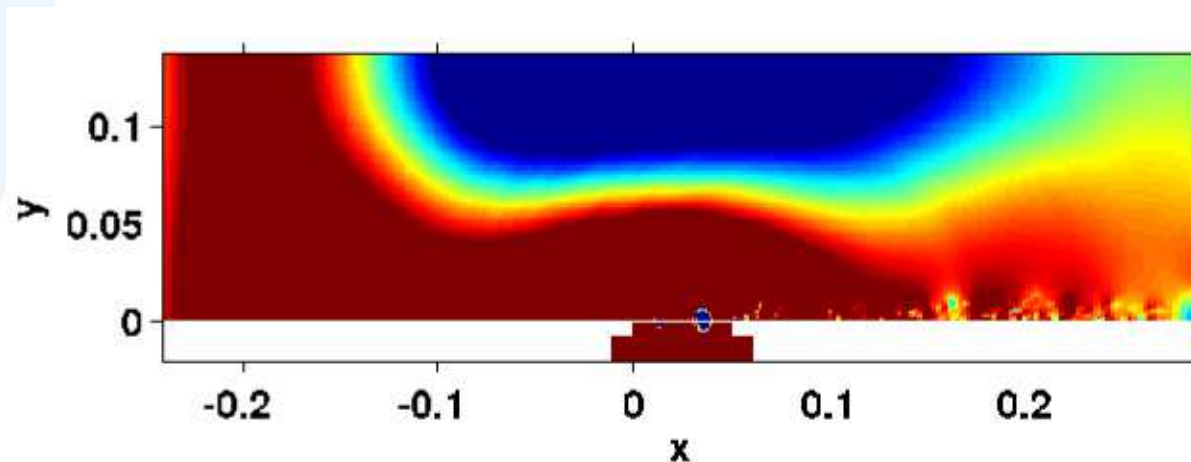
Ducted cavity case (3/4)

© Vorticity in the cavity ($M = 0.18$)

Emmert et al. AIAA Paper 2007, 2008



© Acoustic pressure field in the duct ($M = 0.18$)

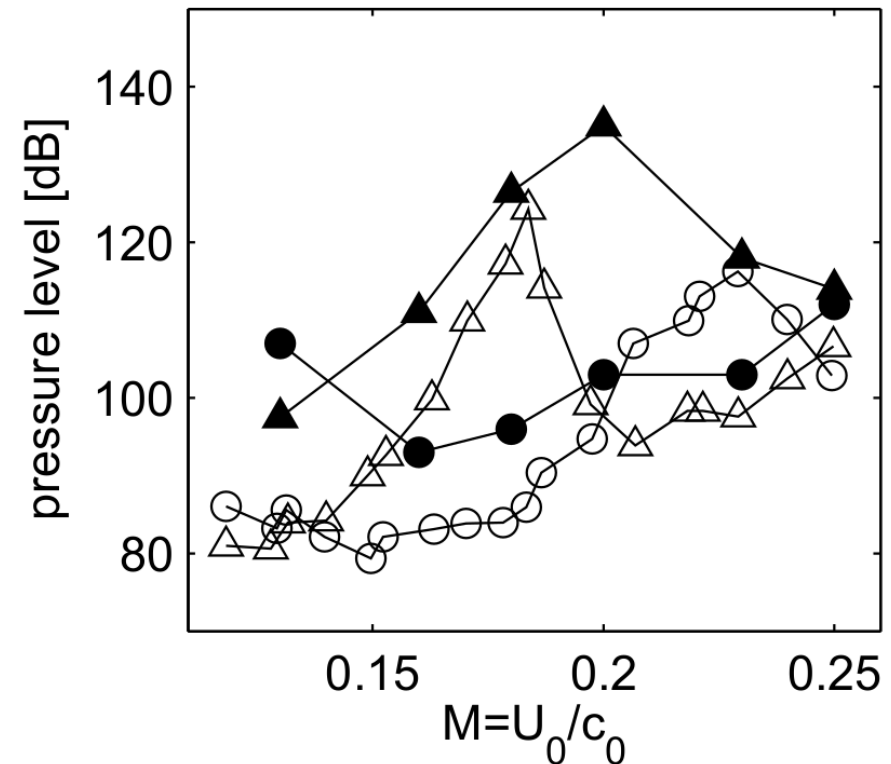
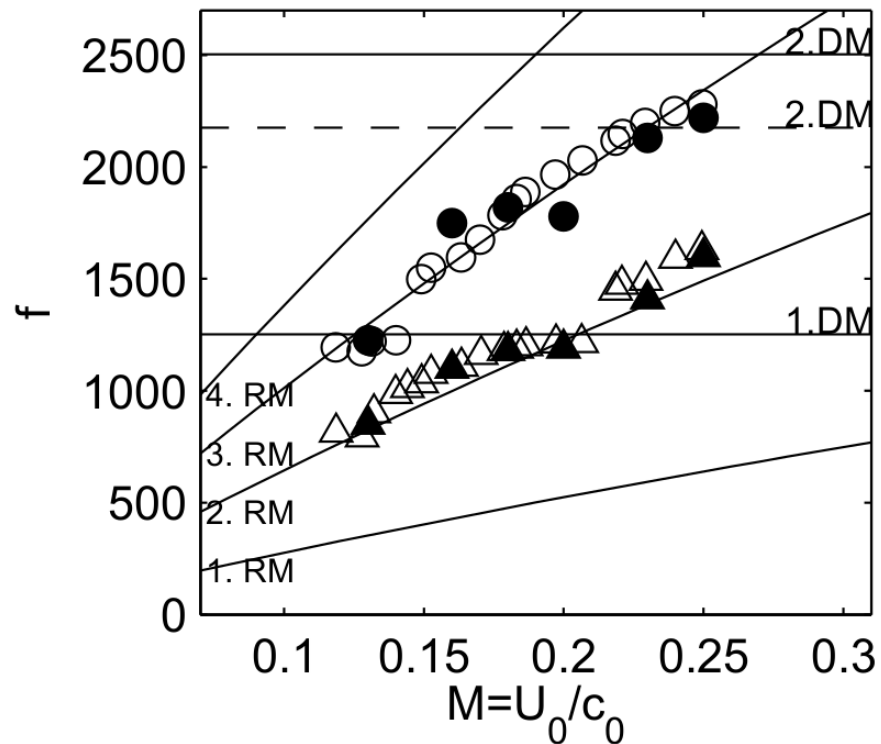




Ducted cavity case (4/4)

Comparisons with experimental results

- Frequencies of the fluctuations in the cavity

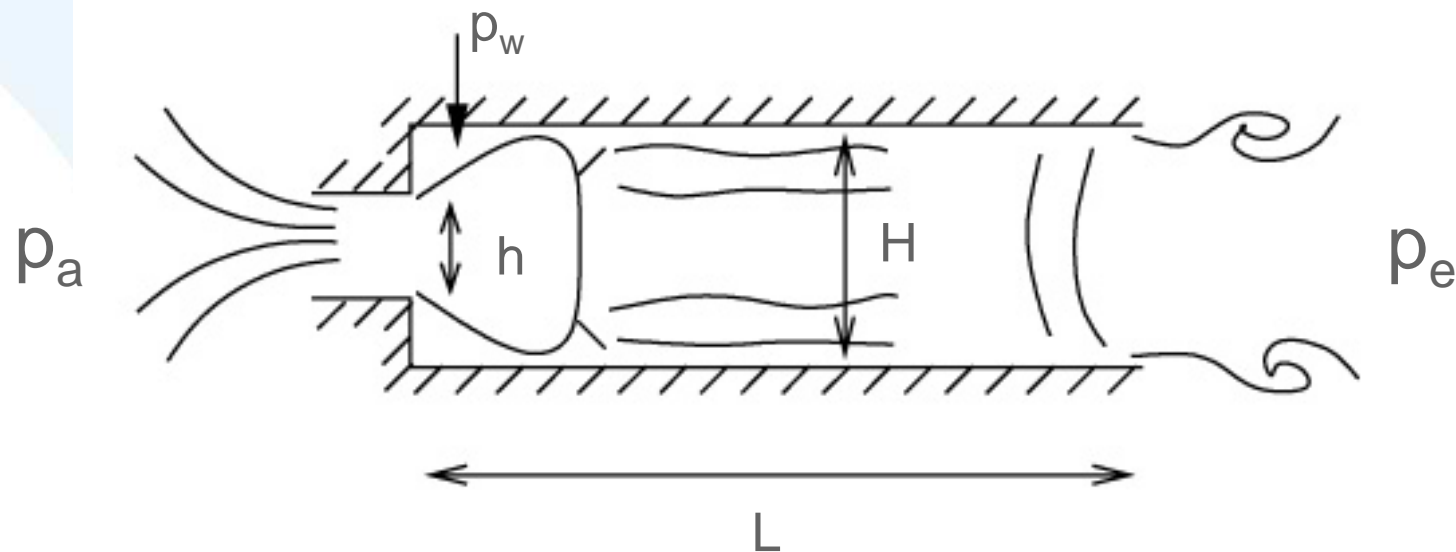


- Pressure level of the fluctuations in the cavity



Sudden enlargement case (1/5)

- Test case typical of the phenomena appearing downstream of high pressure valves in steam duct



$$\begin{aligned} L &= 0.16 \text{ m} \\ L/H &= 4.82 \\ h/H &= 0.3 \end{aligned}$$

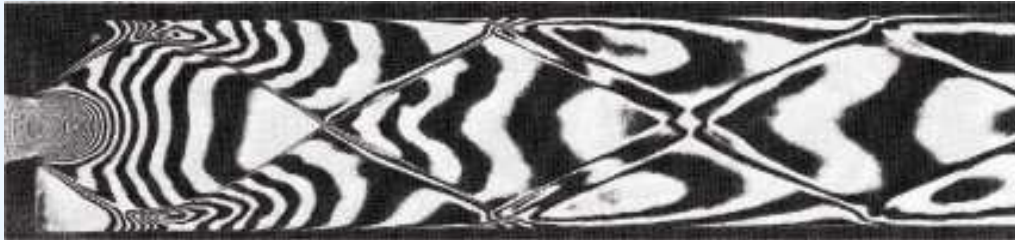
- Flow regimes are driven by the pressure ratio τ

$$\tau = p_e / p_a$$



Sudden enlargement case (2/5)

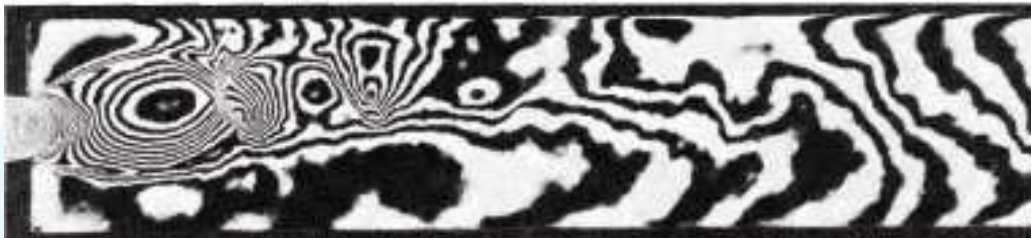
© Experimental data (Anderson et al JFM 1977) : interferometry



$\tau = 0,15$



$\tau = 0,364$



$\tau = 0,377$



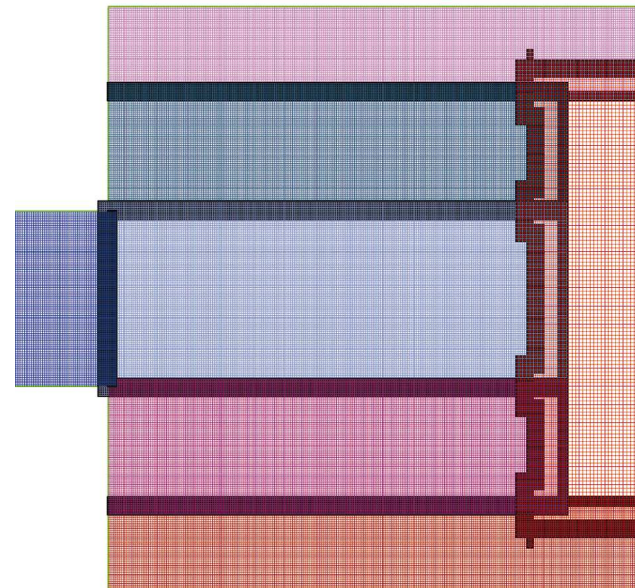
Sudden enlargement case (3/5)

- ◎ Composite grid overview for the supersonic case



- ◎ Grid detail

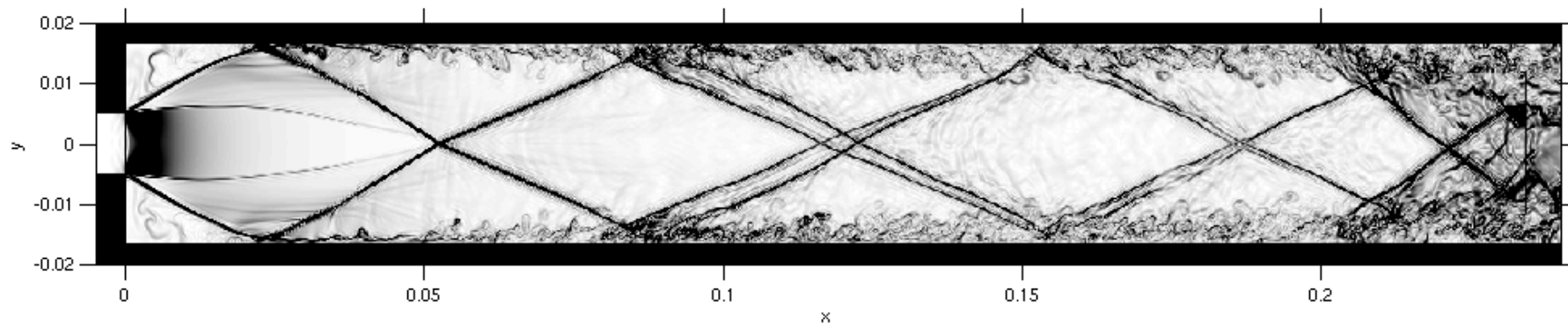
- 15 component grids
- 46 M points
- 253 procs
- $Re_h = 2.1 \cdot 10^5$



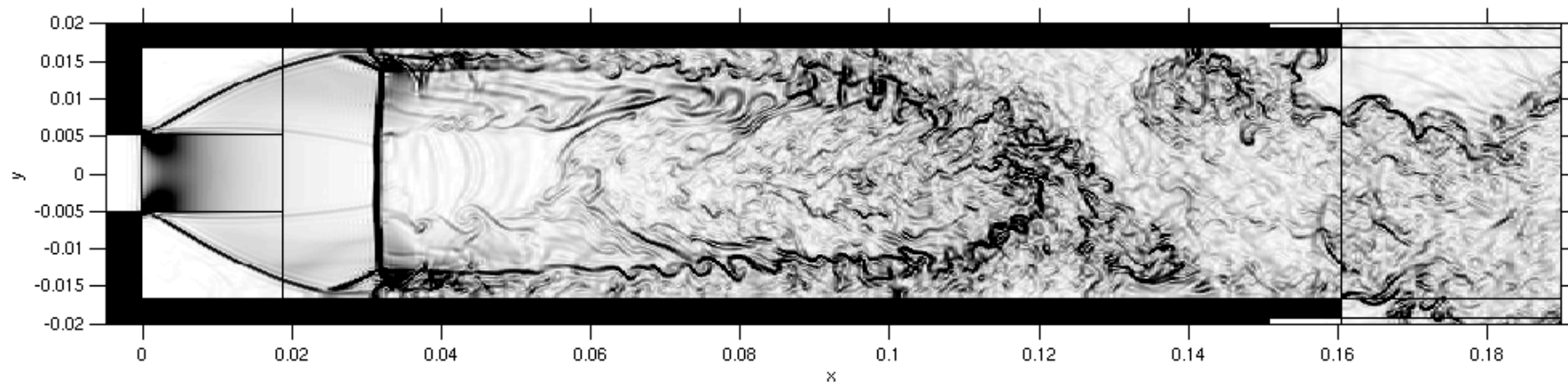


Sudden enlargement case (4/5)

⊙ Supersonic case, $\tau = 0.15$ (numerical Schlieren)



⊙ Transonic case, $\tau = 0.30$ (numerical Schlieren)

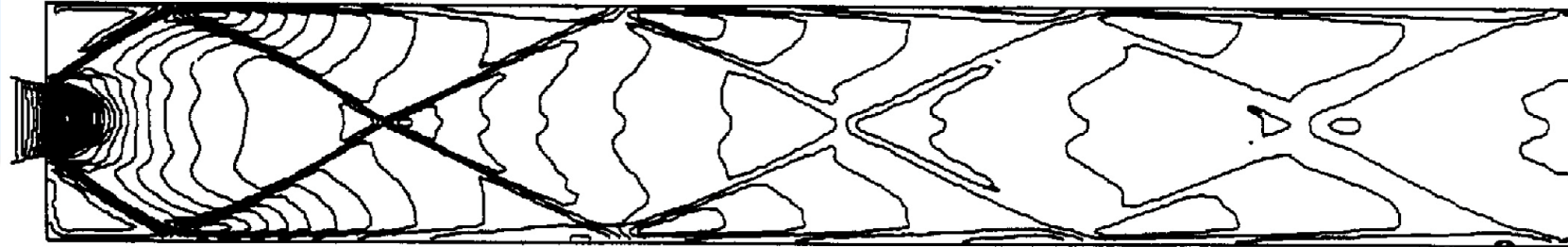


Emmert et al. Phys. Fluids 2009



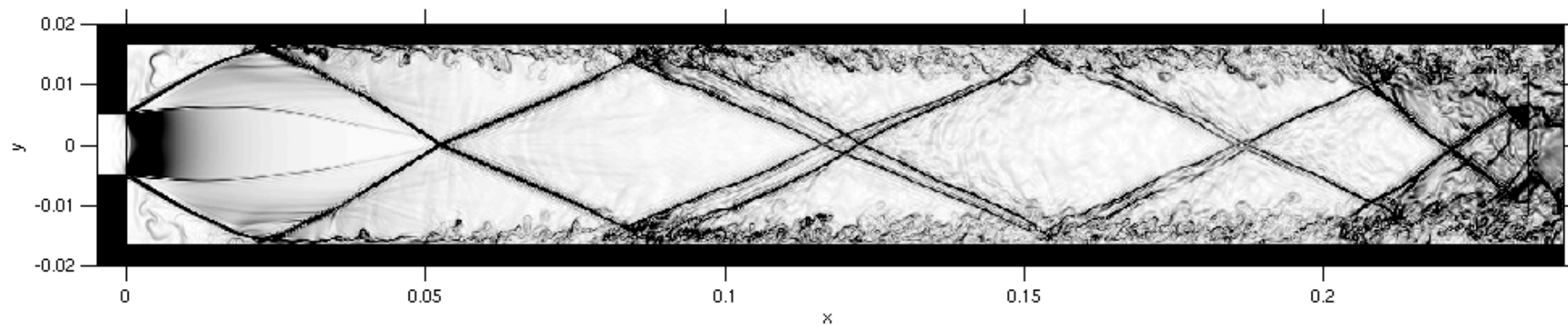
Sudden enlargement case (5/5)

© 1993 : Euler, 2D, 50000 pts



Lafon et al. AIAAP 1993

© 2007 : Navier-Stokes, 3D, 46 M pts

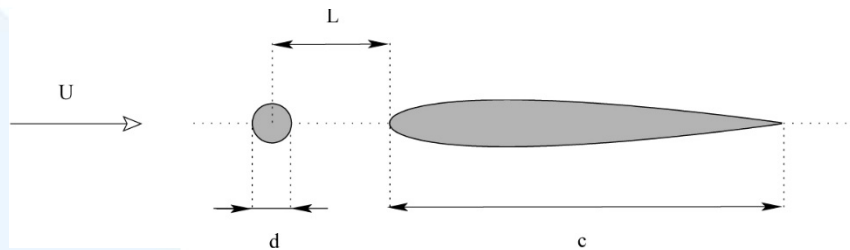


Emmert et al. Phys. Fluids 2009



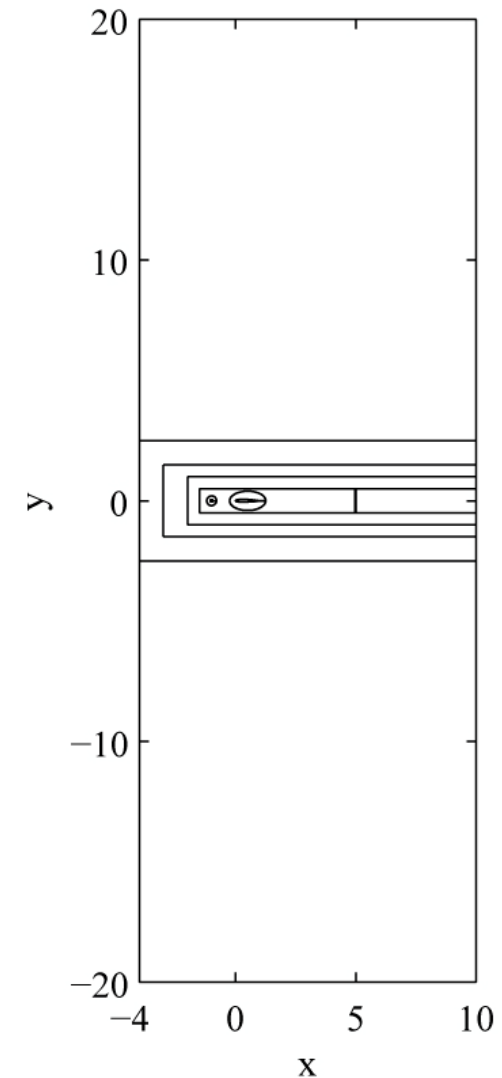
Rod-Airfoil case (1)

◎ Same configuration as Jacob et al. TCFD 2005



◎ Overset composite grid

grid #	type	number of nodes	typical mesh size (m)
1	rod	$500 \times 91 \times 45$	5×10^{-4}
2	airfoil	$400 \times 121 \times 45$	10^{-4}
3	aerodynamic	$1224 \times 189 \times 29$	5×10^{-4}
4	sponge zone	$238 \times 95 \times 29$	10^{-3}
5	intermediate	$1130 \times 189 \times 29$	10^{-3}
6	intermediate	$612 \times 142 \times 15$	2×10^{-3}
7	intermediate	$330 \times 118 \times 8$	4×10^{-3}
8	acoustic	$165 \times 471 \times 4$	10^{-2}

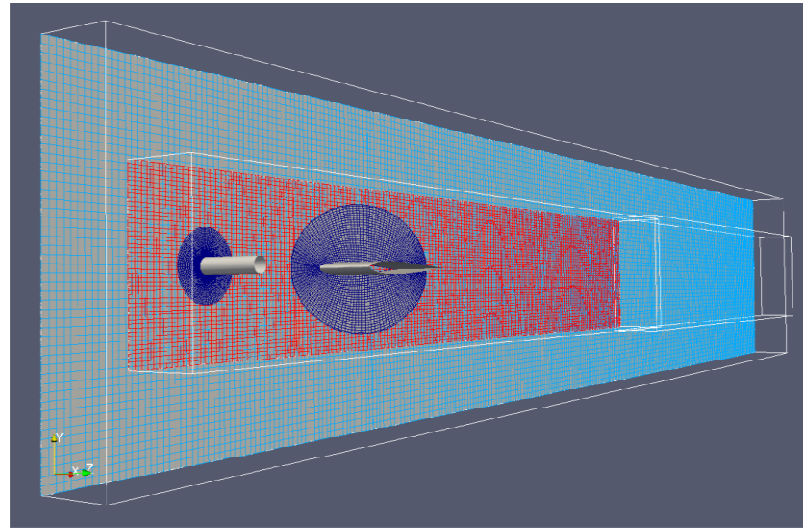


Berland et al. AIAA paper 2010

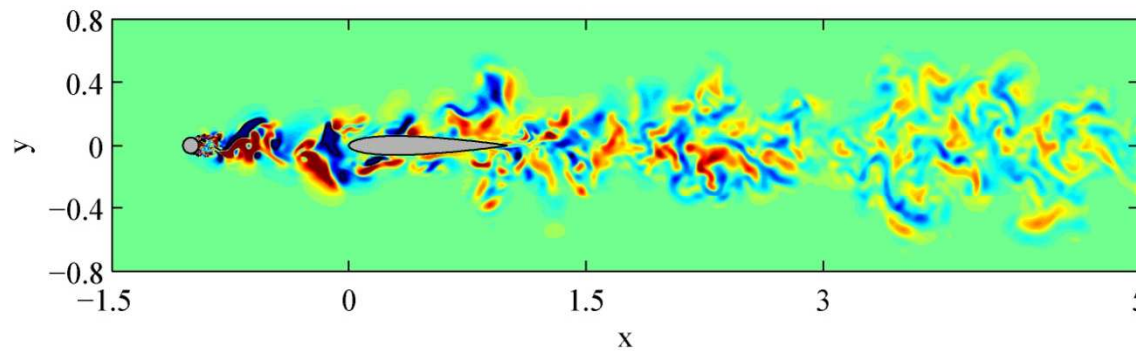


Rod-Airfoil case (2)

Overview of the composite grid (part)



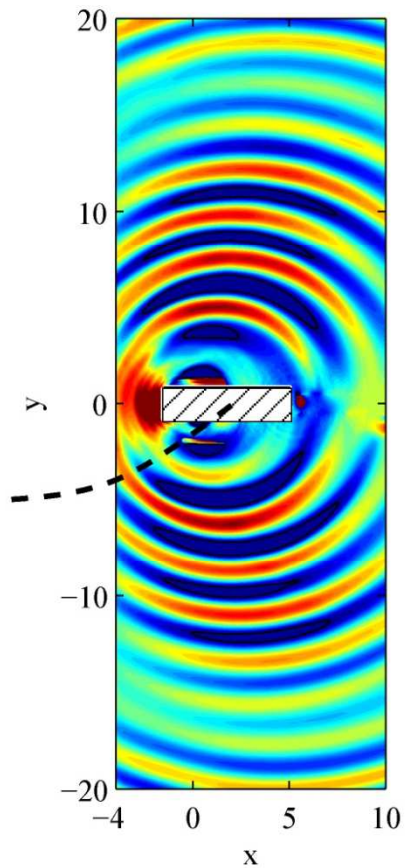
a



Unsteady spanwise velocity field

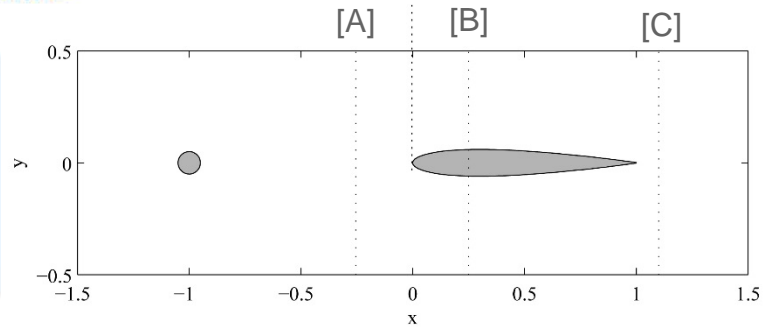
Fluctuating pressure field

b





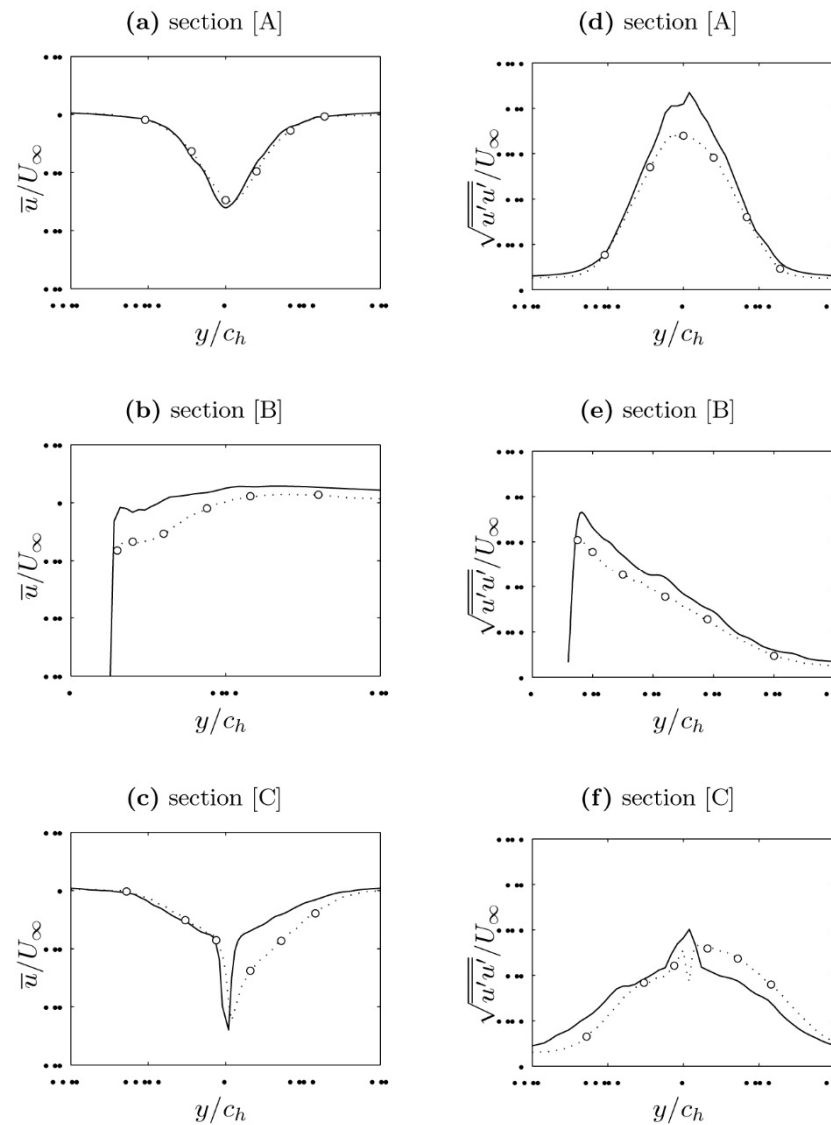
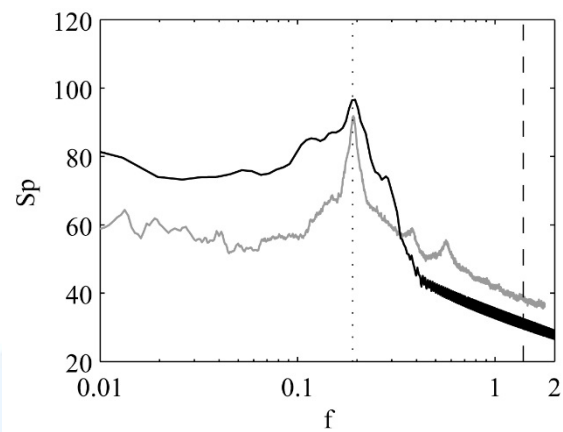
Rod-Airfoil case (3)



Sections [A] [B] [C] for mean streamwise velocity and turbulent intensity comparisons

Experimental results: Jacob et al. TCFD 2005

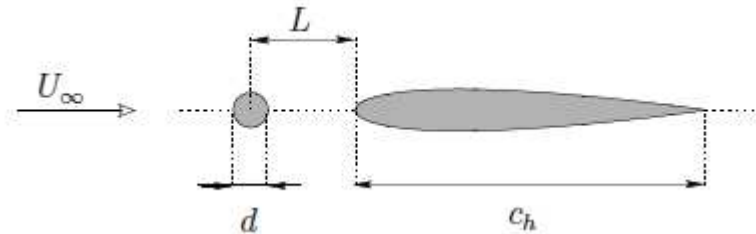
Far field pressure spectrum





Rod-Airfoil case (4)

- ⊙ **Parametric study** on the distance L between the rod and the airfoil
- ⊙ Modification is straightforward with overlapping grids



- ⊙ Several configurations $L/d = 0.7, 1., 1.5, 2.5, 3., 3.5, 4., 5., 6.5, 7., 7.5, 10., 10.5, 14., 17.5$
- ⊙ **Investigation of the influence of the gap L/d** between the rod and the airfoil on the aerodynamic and acoustic field



Rod-Airfoil case (5)

Snapshots of the modulus of the spanwise vorticity

⊙ For small spacings

Shear mode

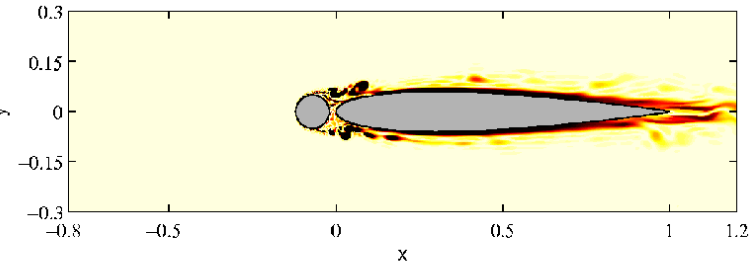
- ✓ The shear layers reattach on the airfoil
- ✓ Flow develops around a « rod-airfoil » body

⊙ For large spacings:

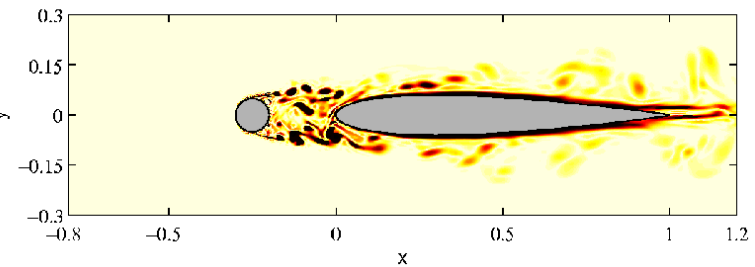
Wake mode

- ✓ The airfoil is in the wake of the cylinder

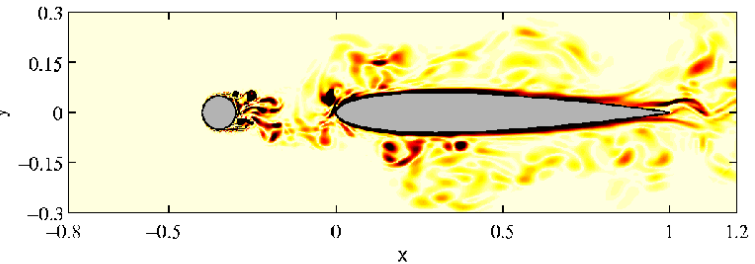
$L/d = 0.7$



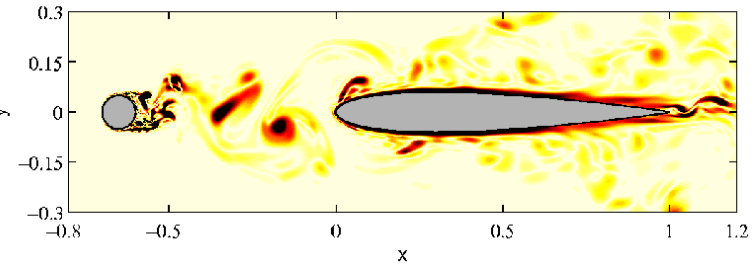
$L/d = 2.5$



$L/d = 3.5$



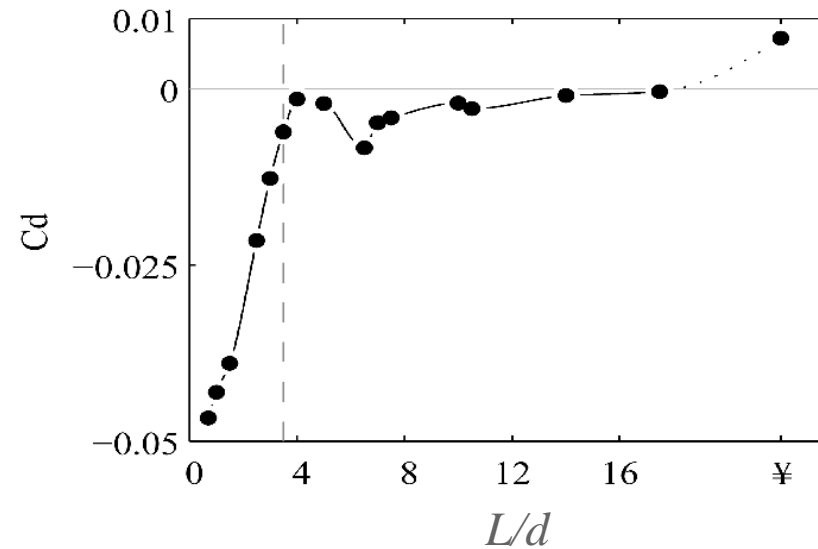
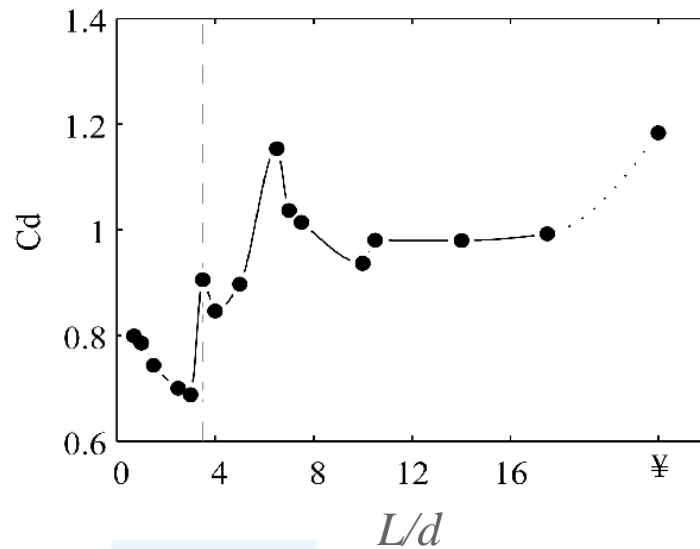
$L/d = 6.5$





Rod-Airfoil case (6)

Drag coefficients of the rod and the airfoil as functions of the distance L/d

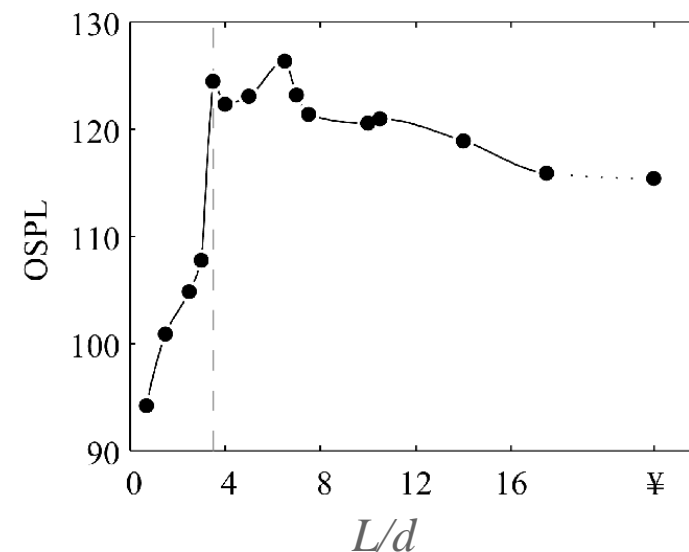
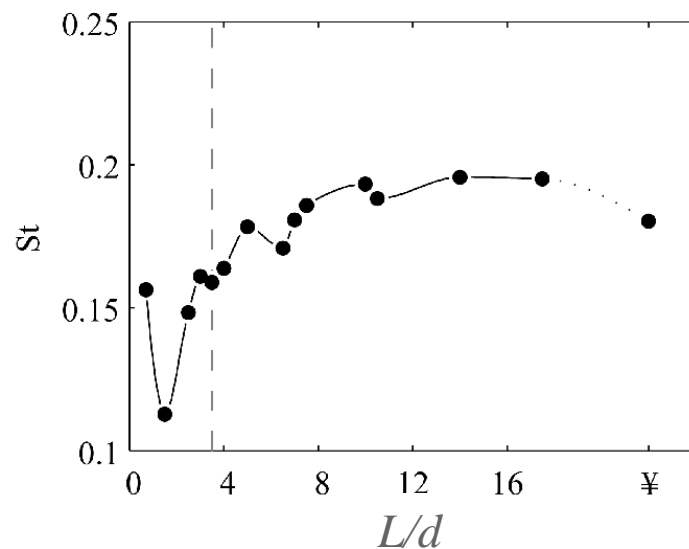


- ✓ The transition between “shear mode” and “wake mode” occurs between the gap values of 3. and 3.5
- ✓ The gap value of 6.5 exhibits a peak value of the drag on the rod
- ✓ The drag of the airfoil is always negative due to the presence of the rod



Rod-Airfoil case (7)

Strouhal number and overall sound power level of the acoustic far field as functions of the distance L/d



- ✓ The two gap values of 3.5 (flow regimes transition) and 6.5 (peak of drag on the rod) produce the highest levels
- ✓ In the wake mode, adding the airfoil makes the flow noisier than for a cylinder alone. It is the contrary in the shear mode



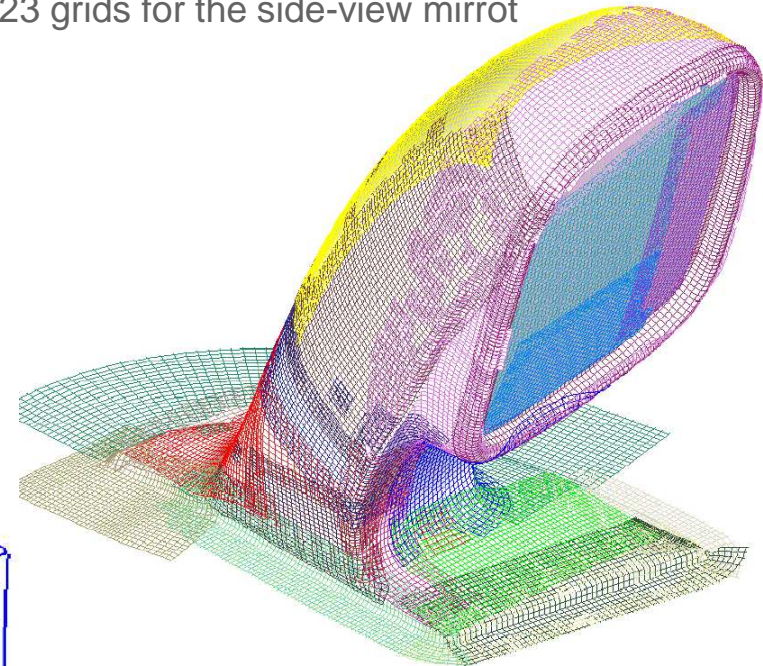
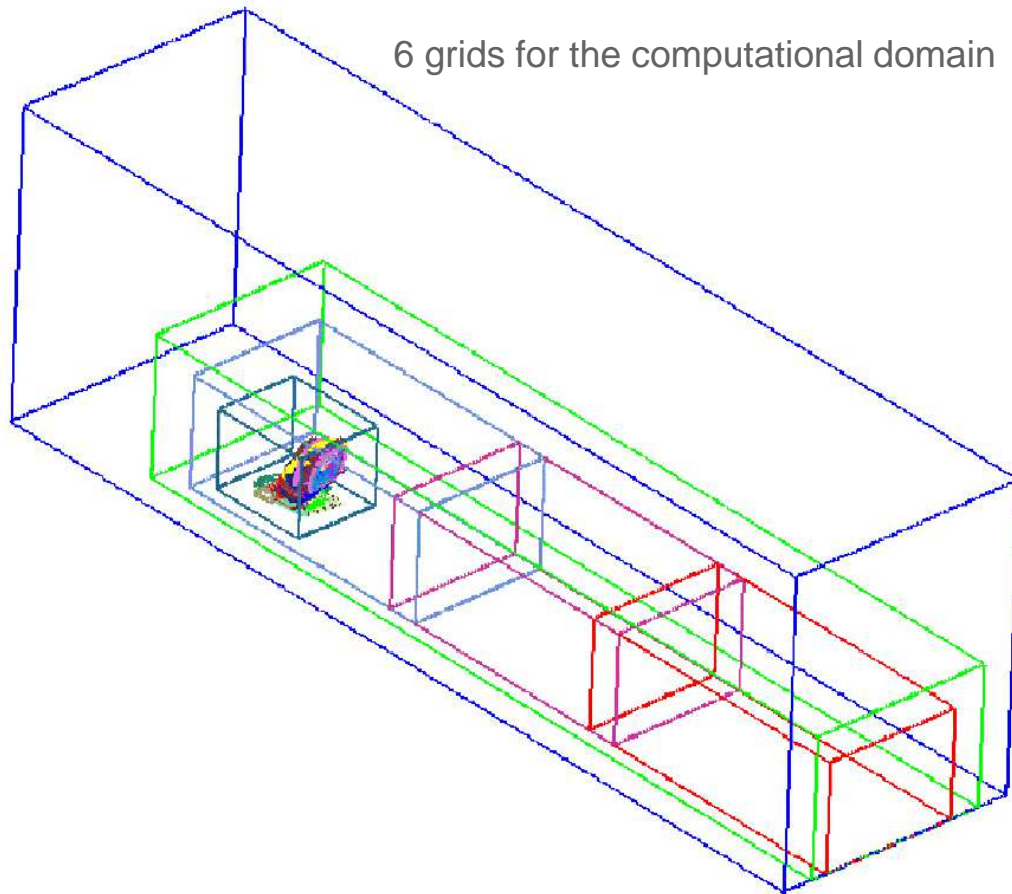
Side-View Mirror Case (1/8)

EDF / PSA Peugeot Citroen collaboration with Dr François Van Herpe

Overview of the grids

23 grids for the side-view mirror

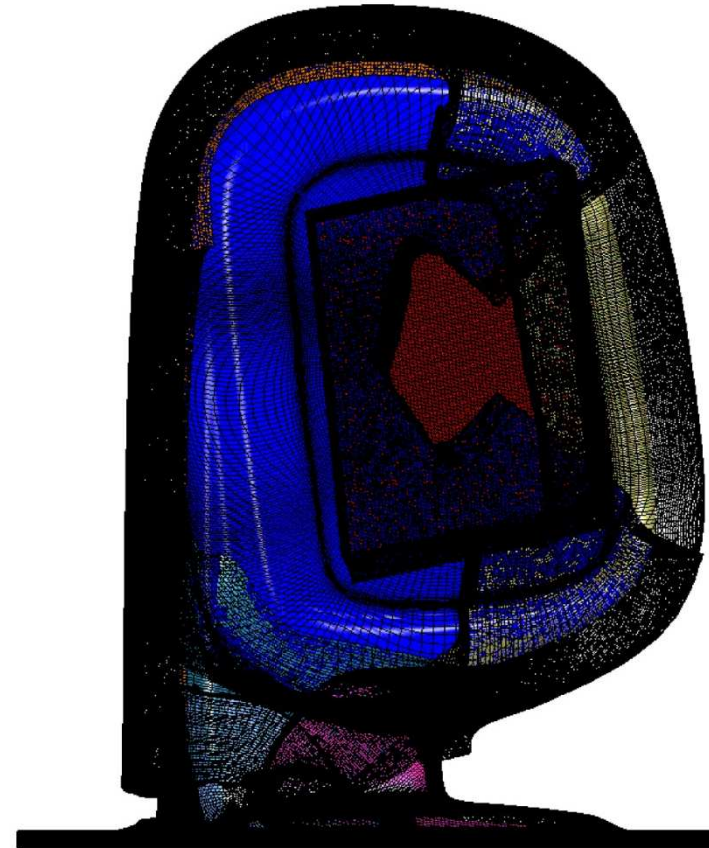
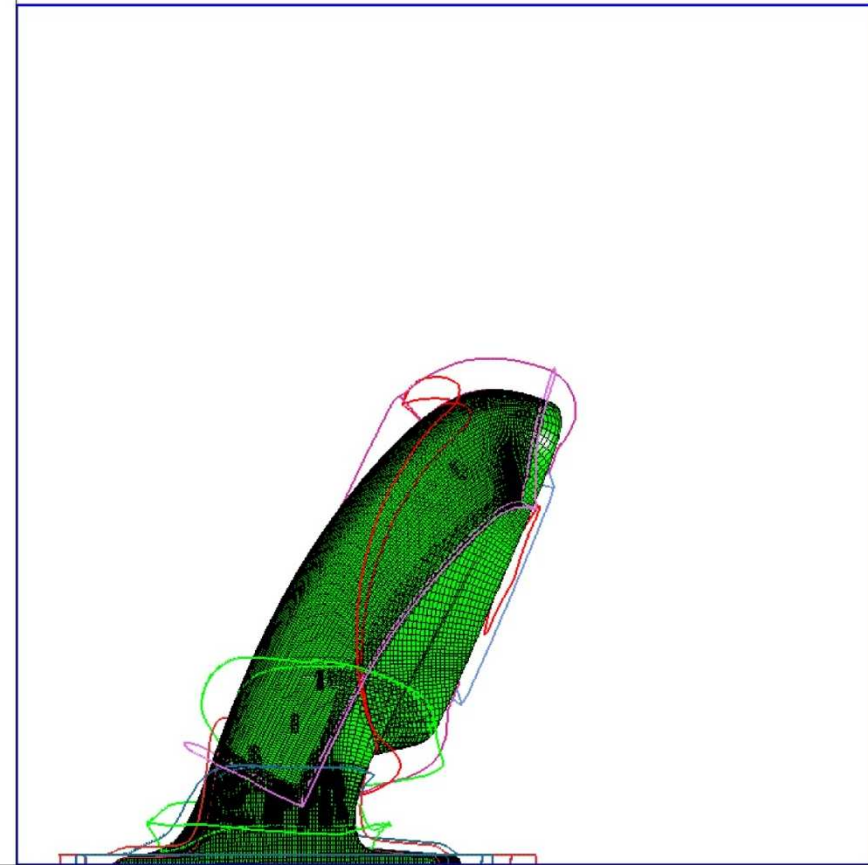
6 grids for the computational domain





Side-View Mirror Case (2/8)

- ◎ Surface and volume grids for the side-view mirror

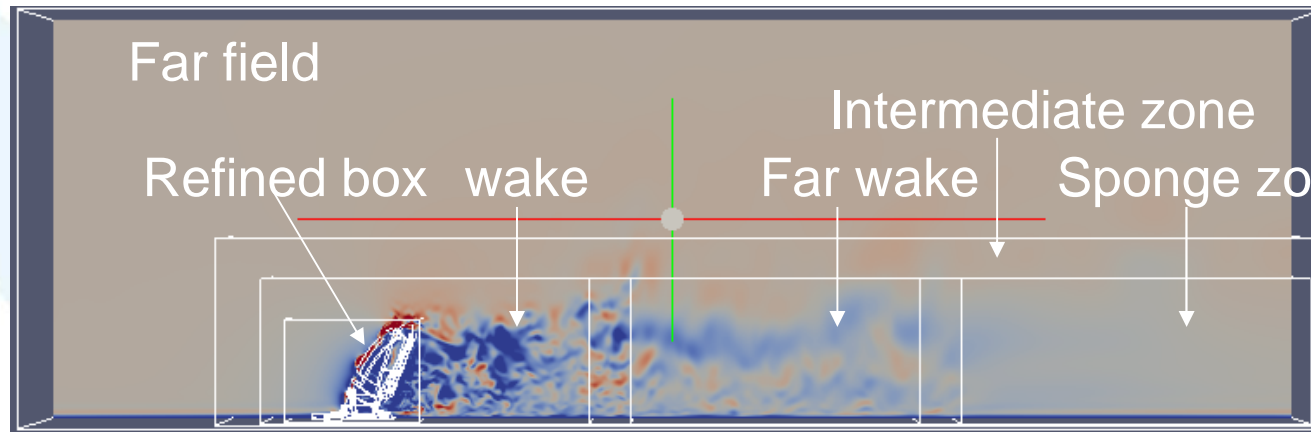




Side-View Mirror Case (3/8)

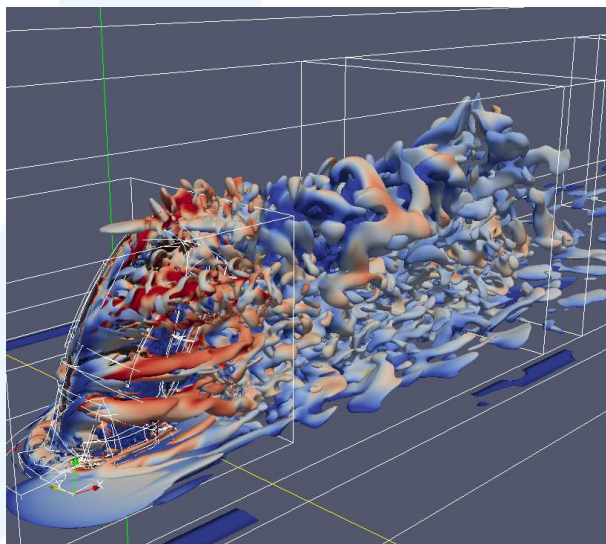
Velocity magnitude

Van Herpe et al. AIAA paper 2011



$U_\infty = 40 \text{ m/s}$
 $\Delta t = 0.34 \times 10^{-6} \text{ s}$
 $\text{CFL} = 0.9$

Swirl contour



	N_x	N_y	N_z	N_{tot}	N_{procs}
Refined box	330	270	250	34375	648
Wake	480	230	180	33392	588
Far wake	480	115	90	31764	153
Sponge zone	240	115	90	29936	81
Intermediate zone	665	150	115	33567	336
Far field	390	100	125	33162	144

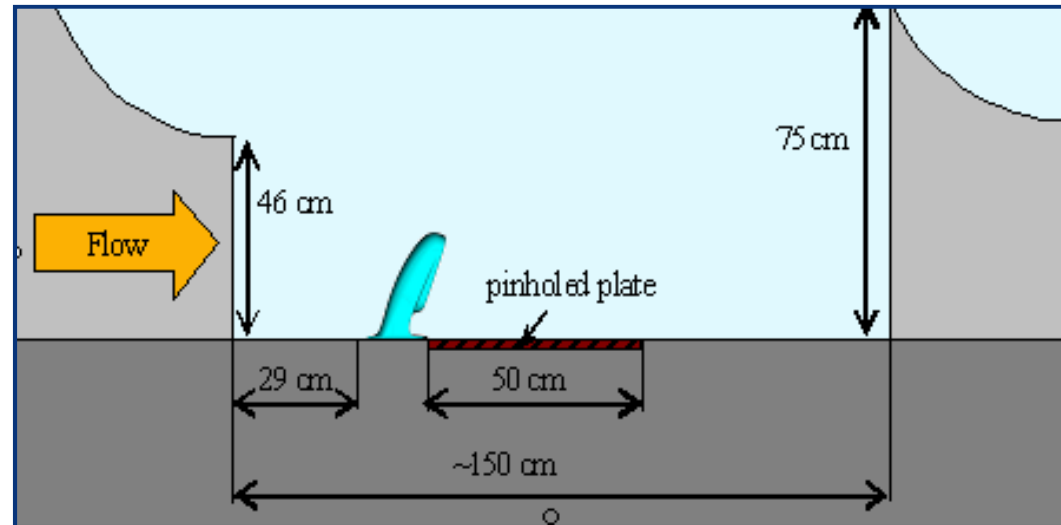
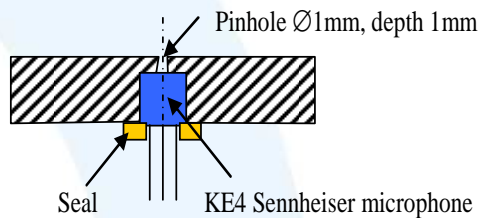
Total number of grid points $\sim 65 \times 10^6$



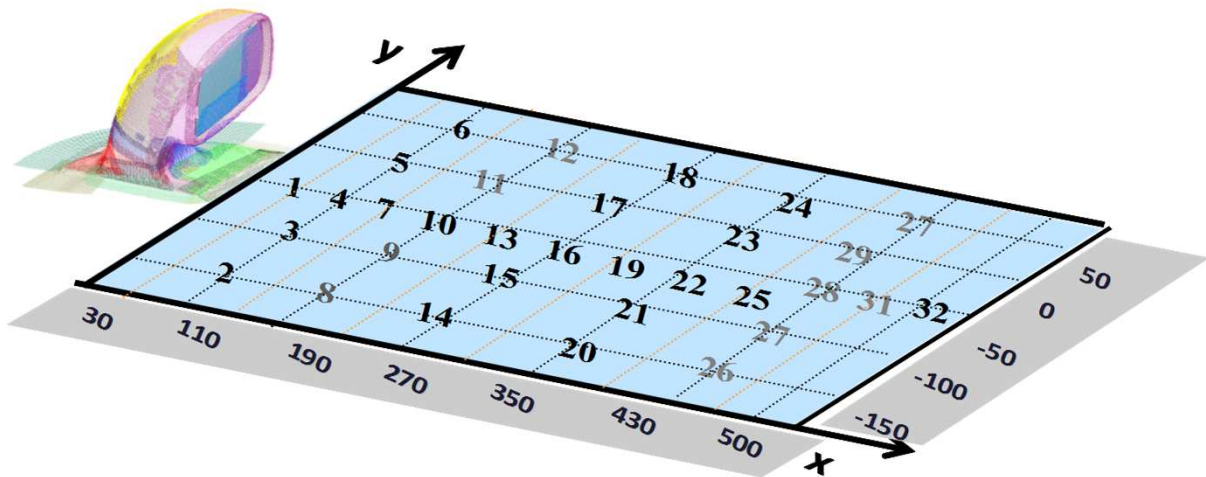
Side-View Mirror Case (4/8)

Experimental set-up

- Anechoic wind tunnel
- Pinhole microphones



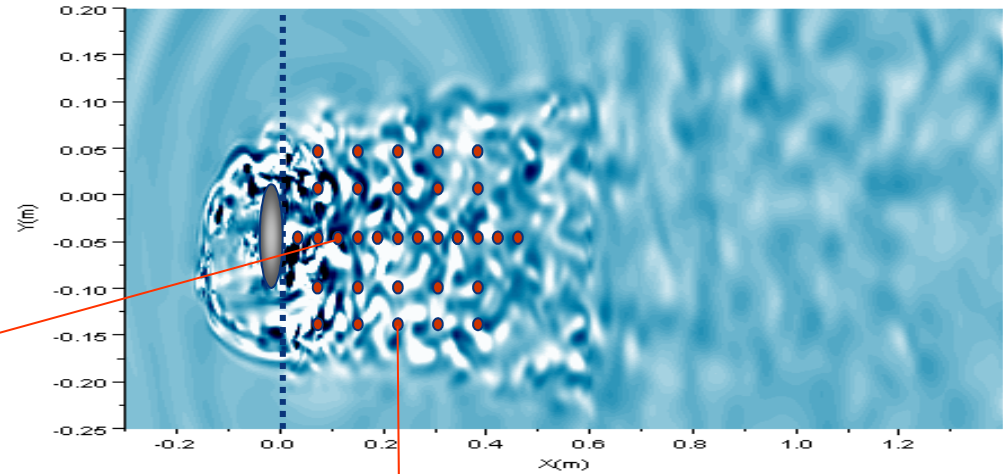
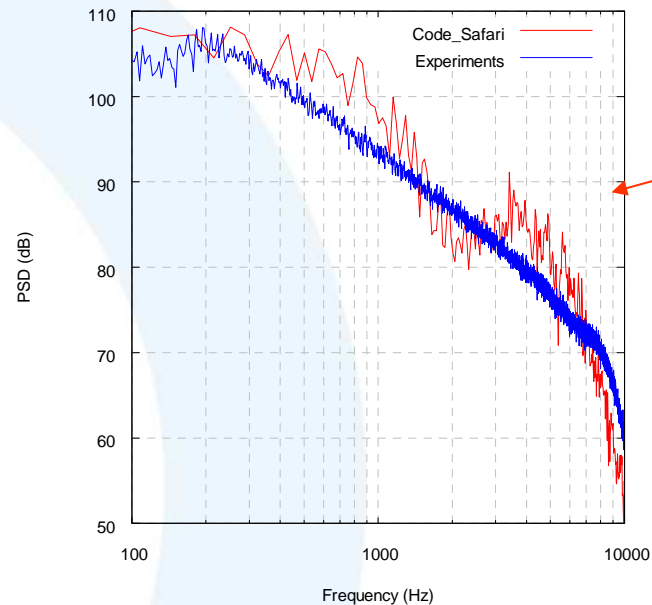
Comparison points



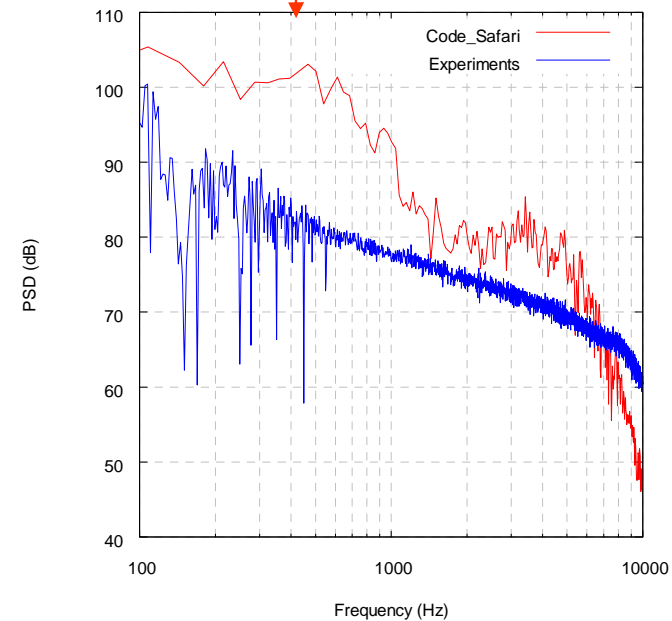


Side-View Mirror Case (5/8)

◎ Good correlation in the middle of the wake



- ◎ The correlation is not good
 - Outside of the middle of the wake
 - At low frequencies ($f < 1$ kHz)

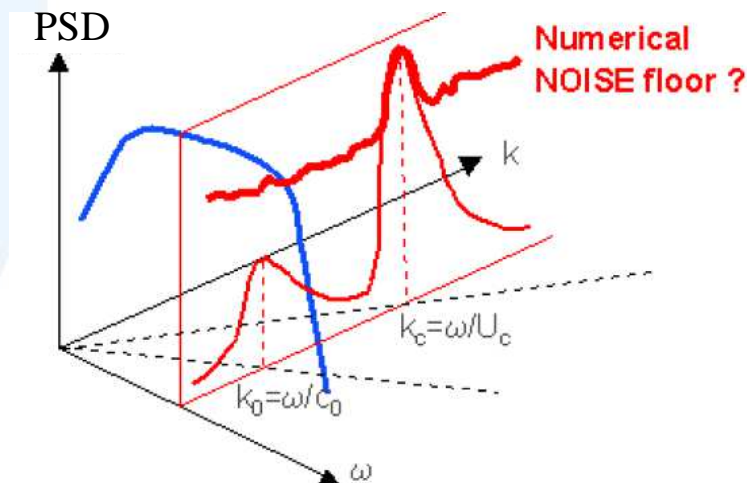




Side-View Mirror Case (6/8)

Frequency wave number separation

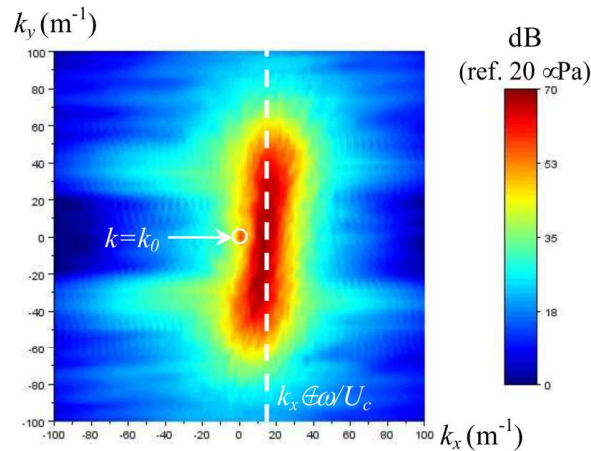
- ◎ Sound velocity $c_0 \gg U_c$ pseudo-sound convection velocity
- ◎ Convected wavenumber $k_c = \omega/U_c \gg k_0 = \omega/c_0$ acoustic wavenumber
- ◎ 2 distinct peaks on a $k-\omega$ graph of the WPF
 - Magnitude of the convective peak \gg Magnitude of the acoustic peak



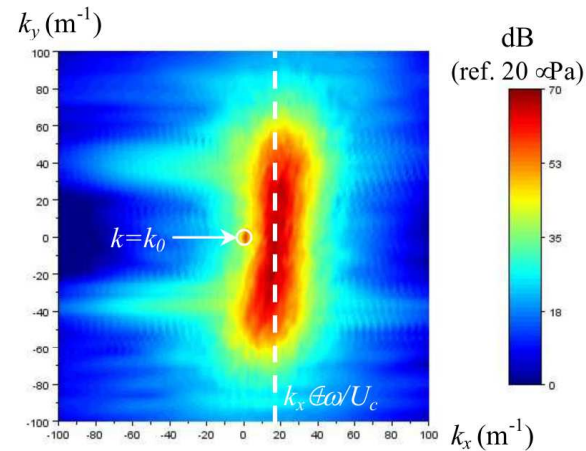


Side-View Mirror Case (7/8)

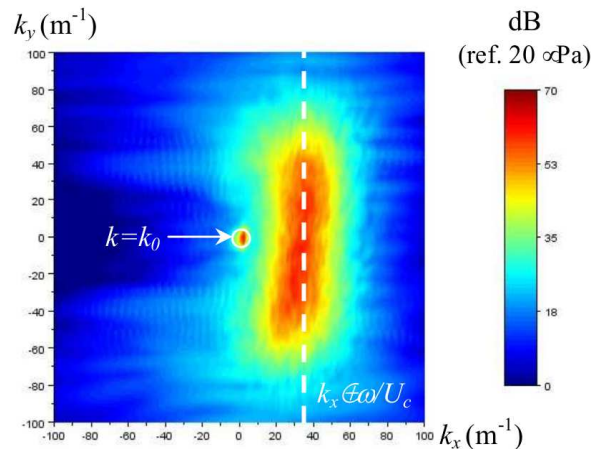
- Sound and pseudo-sound patterns are detected on k_x - k_y diagram
 - Acoustic spot: $k_x^2 + k_y^2 \leq (\omega/c_0)^2$ and Convective line $k_x \sim \omega/U_c$



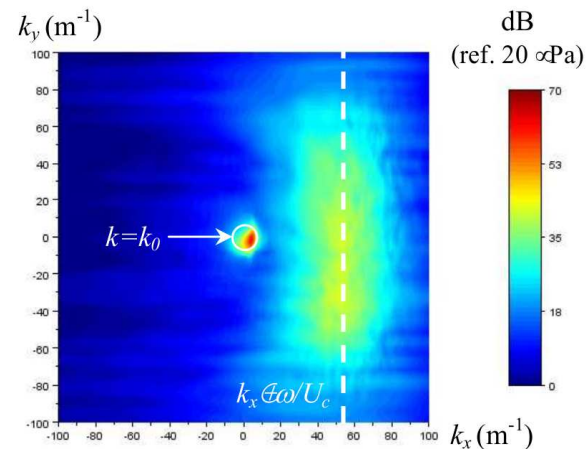
a) 400 Hz



b) 500 Hz



a) 1000 Hz



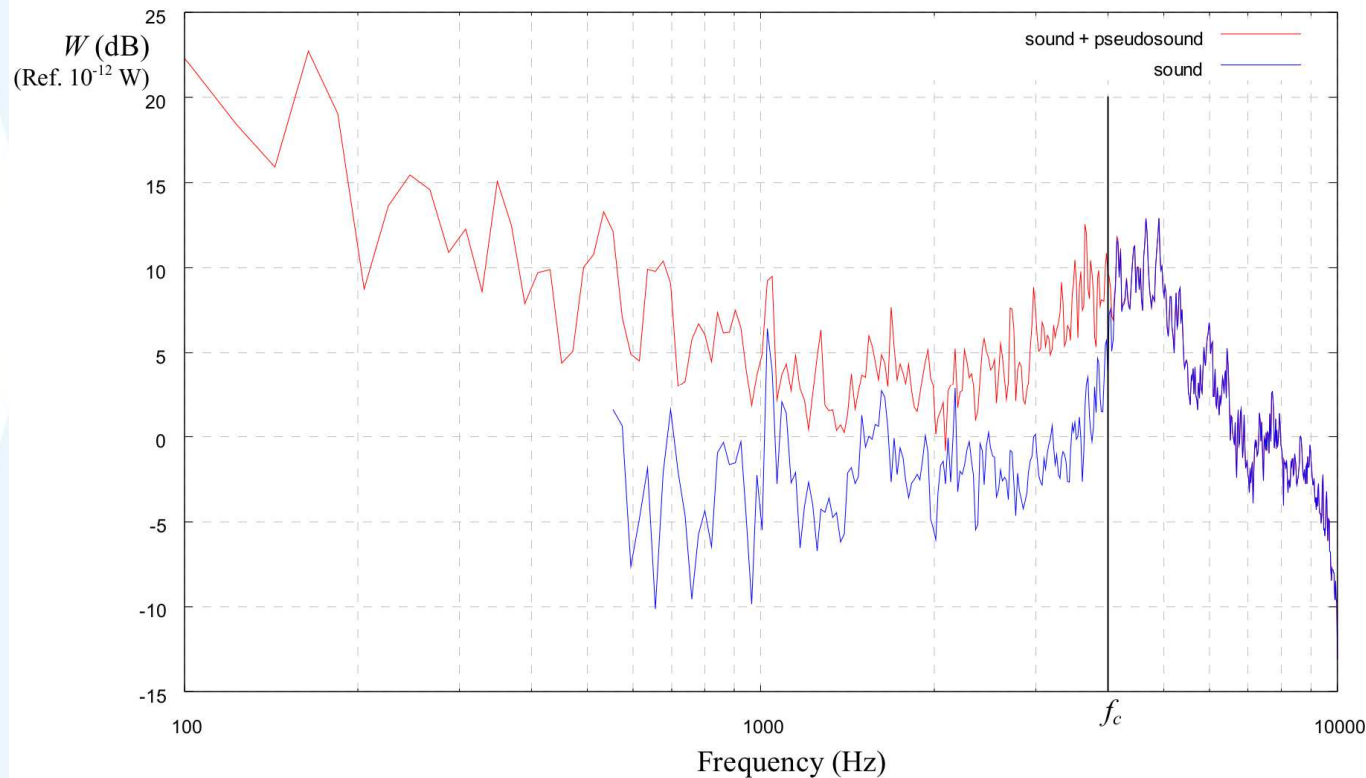
b) 2000 Hz



Side-View Mirror Case (8/8)

- Based on these results, different vibroacoustic approaches can be applied on both the sound fluctuations and the pseudosound fluctuations recorded on the side window due to the side-view mirror and can be used to evaluate their respective contribution to the interior noise

Van Herpe et al. AIAA paper 2012

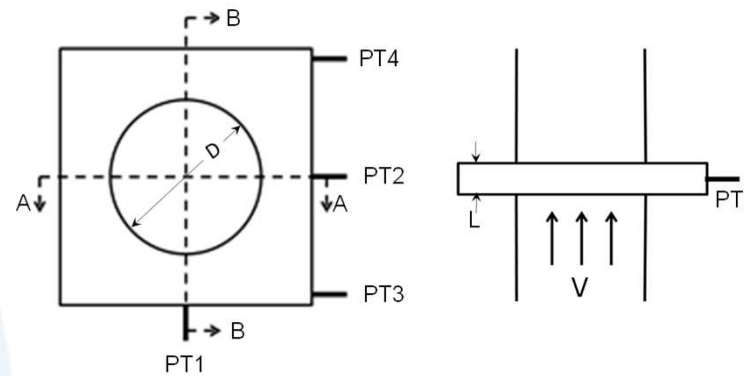




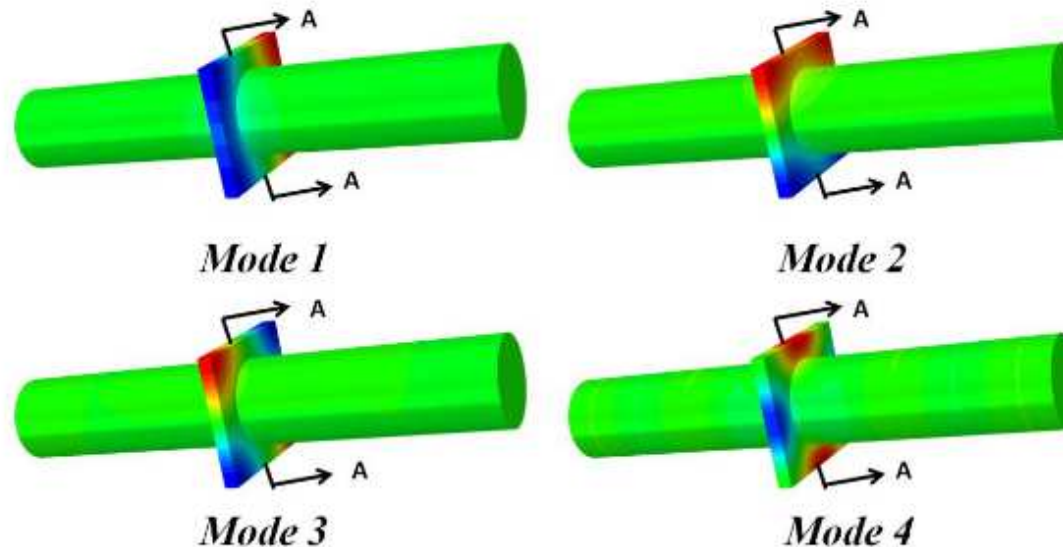
New case : square ducted cavity (1/2)

EDF / McMaster Univ. collaboration with Pr Samir Ziada

- Trapped acoustic modes in a square ducted cavity



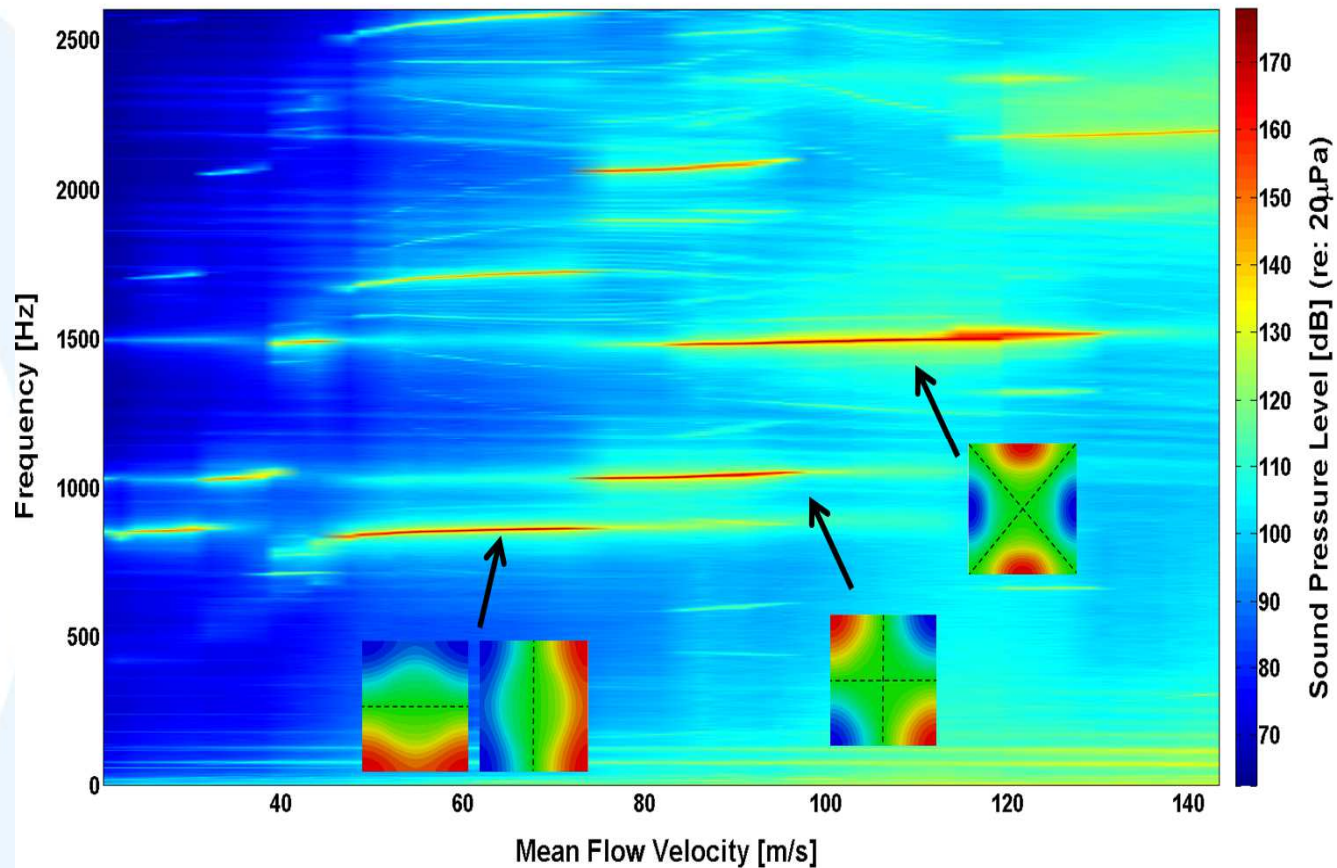
- Mode shapes





New case : square ducted cavity (2/2)

© Aeroacoustic response of the cavity



Bolduc et al. AIAAJ 2016
Ziada et al JSV (to be submitted)



Numerical method for multiphysics (1/4)

⊙ Needs of new numerical methods for new multiphysics application

- Transients in two phase flow

- Shock waves, contact discontinuities, vaporization wave

- Importance of variable positivity

⊙ Euler + species transport

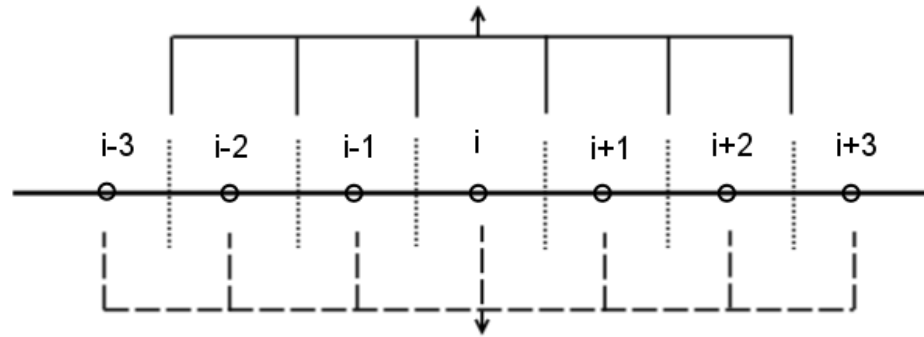
$$\begin{cases} \frac{\partial \mathbf{W}}{\partial t} + \frac{\partial \mathbf{F}(\mathbf{W})}{\partial x} = 0 \\ \frac{\partial (\rho Y_i)}{\partial t} + \frac{\partial (\rho u Y_i)}{\partial x} = 0 \end{cases}$$



Numerical method for multiphysics (2/4)

- High order hyperbolic method (Nonomura et al. JCP 2012)

$$\left. \frac{\partial \mathbf{F}(\mathbf{W})}{\partial x} \right|_{x=x_i} = \frac{1}{\Delta x} \sum_{k=1}^3 \alpha_k (\mathbf{F}_{i+k-1/2} - \mathbf{F}_{i-k+1/2})$$



WENO interpolation

$$\mathbf{W}_{i+1/2}^-, \mathbf{W}_{i+1/2}^+$$

HLLC Riemann Solver

$$\longrightarrow \mathbf{F}_{i+1/2} \longrightarrow$$

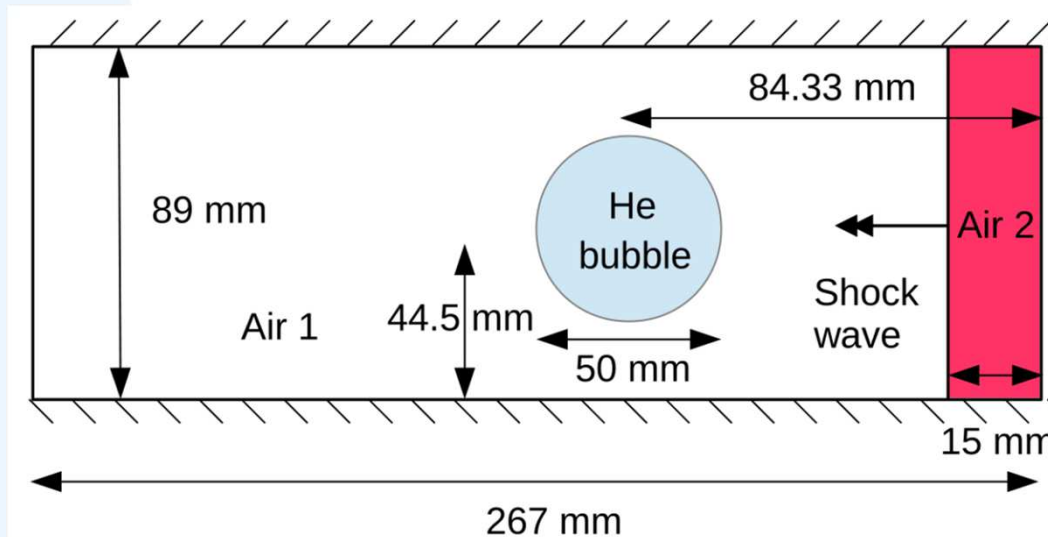
$$\left. \frac{\partial \mathbf{F}(\mathbf{W})}{\partial x} \right|_{x=x_i}$$



Numerical method for multiphysics (3/4)

● Shock wave / He Bubble interaction test case

- A Mach 1.22 shock wave goes through a Helium bubble in air medium at rest
- Experiments
 - Haas & Sturtevant JFM 1987
- Definition of the test case

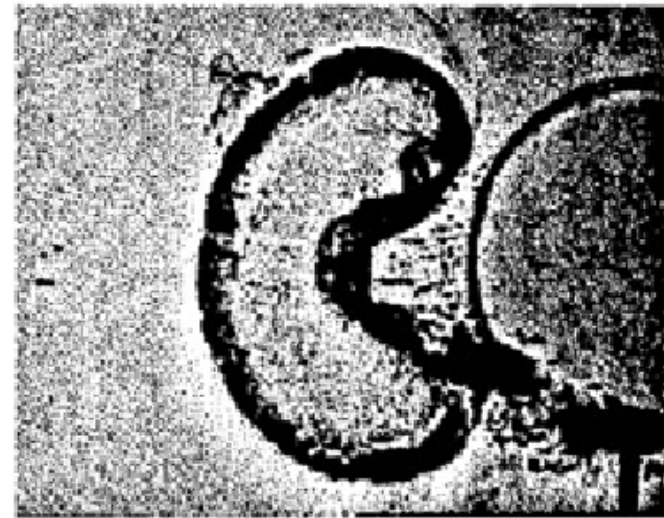
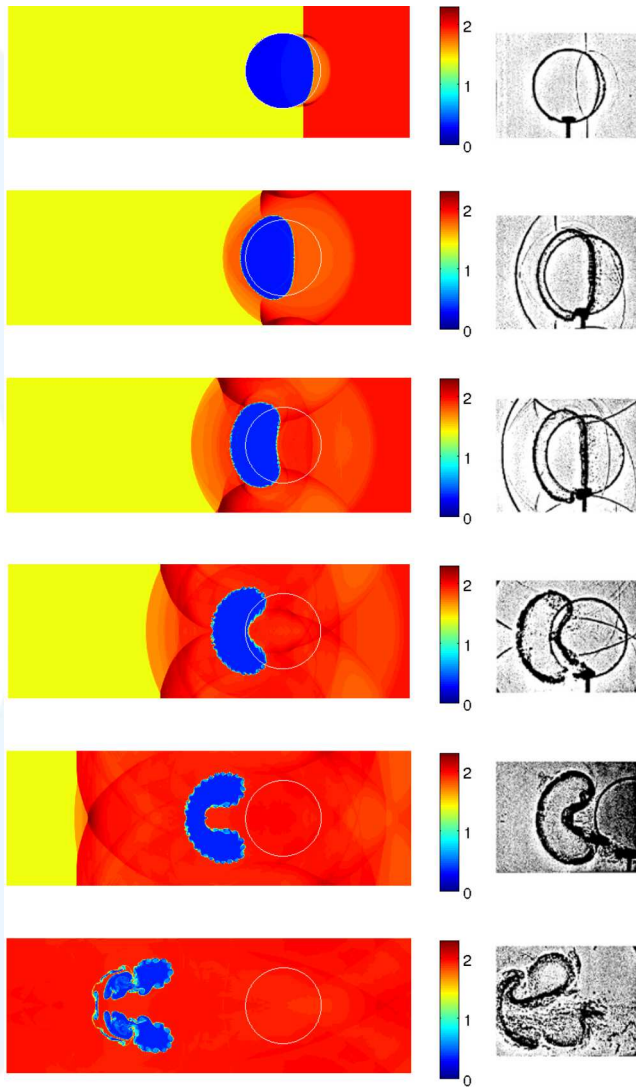


- From Daude et al. Computers and Fluids 2012

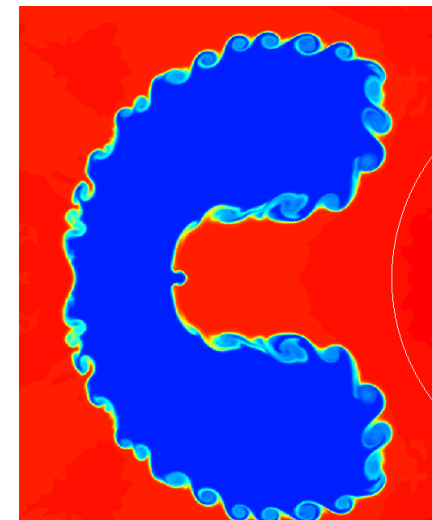


Numerical method for multiphysics (4/4)

© Comparison of numerical and experimental snapshots



Density fields





Conclusion

- ◎ Code_Safari, a high order numerical tool for CAA, has been developed
- ◎ Tests and validations have been carried out for EDF main applications of industrial interests:
 - Unsteady compressible flows
 - Flow/acoustics interactions
- ◎ Others capabilities are available
 - Moving grids for aeroelasticity
 - Linear frequency solver
 - Complex impedance for outdoors acoustic propagation
- ◎ The main objective is to have an expertise tool in order to be able to help analysing industrial problems



Acknowledgements

- ◎ Thomas Emmert, Julien Berland, Frédéric Daude, Fabien Crouzet, Romain Lacombe, *EDF R&D, France*
- ◎ Sébastien Candell, *Ecole Centrale Paris*
- ◎ Christophe Bailly, Christophe Bogey, Olivier Marsden, *Ecole Centrale Lyon, France*
- ◎ François Van Herpe, *PSA Peugeot Citroen, France*
- ◎ Bill Henshaw, *Lawrence Livermore Laboratory, USA*
- ◎ Samir Ziada, *McMaster University, Canada*